

Rheodielectric study on shear-induced structural change in the smectic-A phase of 4-*n*-octyl-4'-cyanobiphenyl (8CB)

K. Negita and H. Kaneko

Department of Chemistry, Faculty of Science, Fukuoka University, Nanakuma 8-19-1, Jonan-ku, Fukuoka 814-0180, Japan

(Received 11 April 2009; published 20 July 2009)

Simultaneous measurements of rheological and dielectric properties are made to investigate shear-induced structural change in the smectic-A phase of 8CB (4-*n*-octyl-4'-cyanobiphenyl). With increasing the shear rate, the fluidity changes from non-Newtonian to Newtonian flow via an unstable flow region, accompanied by a characteristic change in the dielectric permittivity. In the non-Newtonian flow region, a dielectric dispersion, which can be ascribed to an undulation motion of smectic layer, is recognized. On the basis of these results, it is suggested that with increasing the shear rate the undulation changes to a chaotic structure, which is followed by a more simple structure with the layer normal along the neutral axis, and that these structural changes are responsible for the fluidity change.

DOI: [10.1103/PhysRevE.80.011705](https://doi.org/10.1103/PhysRevE.80.011705)

PACS number(s): 83.80.Xz, 64.70.M-, 47.20.Ft, 77.22.Gm

I. INTRODUCTION

In the liquid crystals, various phases (structures) exist depending on the orientational and the positional orders of the molecules. These orders are easily modified if a shear flow is applied, leading to various shear-induced structures [1,2]. In the case of the nematic (*N*) phase, a steady shear flow induces an alignment of the director, a unit vector specifying the averaged direction of the liquid crystalline molecules, near the flow direction [3,4]. Such a behavior has been well studied experimentally and has been understood in terms of the Leslie-Ericksen theory [5,6]. The flow alignment is observed in the whole temperature region of the *N* phase if the materials have a phase sequence of crystal (Cr)–nematic (*N*)–isotropic liquid (*I*) like 4-*n*-pentyl-4'-cyanobiphenyl (5CB) [4,7], while in materials having smectic-A (S_A) phase below the *N* phase, a significant change in the shear-induced structure occurs due to a development of the S_A order [8–16]; the flow alignment in the *N* phase is possible only just below the *N*-*I* phase transition point. In the case of the *N* phase of 8CB, which has a phase sequence of Cr- S_A -*N*-*I*, some precessional motions of the director are excited around the neutral direction when approaching to the S_A -*N* phase transition point T_{AN} ; depending on the temperature and the shear rate, dynamical structures [$a_m, a_s, a(b), a_c$] characterized by different precessional motions are induced [10,11].

In the S_A phase of 8CB, the viscosity largely increases with a decrease in temperature owing to the formation of one-dimensional positional order along the director [13,15]. The steady shear flow affects the structure in this phase as well as in the *N* phase. From the x-ray scattering experiment under shear flow, it is suggested that a structural change occurs if the shear rate is varied [10,11]. As shown in Fig. 1, at lower shear rate, a' - c' structure—which is composed of a' and c' structures—is stable. Here, a' and c' structures are characterized by the director oriented along the neutral and the velocity gradient directions, respectively. While at higher shear rates, the a' - c' structure changes to a' structure, where the director aligns along the neutral direction homogeneously. Some rheological studies have been made on this structural change, showing that the flow is non-Newtonian in

the a' - c' region, while it is Newtonian in the a' region [13–16]. Although the a' structure is simple enough to understand, with respect to a' - c' , it is not well clarified how the a' structure mixes with the c' structure. Panizza *et al.* [16] suggested from the x-ray scattering that a structure composed of multilamellar cylinders oriented along the flow direction corresponds to the a' - c' structure. On the other hand, our preliminary study shows a possibility that the a' - c' structure is characterized by a shear-induced undulation [15]. The undulation instability induced by the shear flow has been studied in the layered systems including lyotropic lamellar and the thermotropic smectic phases [17–22], showing that the shear-induced change from the c' to the a' structure, which is sometimes called parallel to perpendicular change, is associated with the undulation instability. In the present study, simultaneous rheological and dielectric measurements are made in detail to shed light on the shear-induced structural change in the S_A phase of 8CB.

II. EXPERIMENT

The liquid crystalline specimen 8CB was obtained from Merck Co. and was used without further purification. The rheological and the dielectric properties were measured simultaneously with a concentric double-cylinder viscometer. For the measurements of the shear-modified dielectric per-

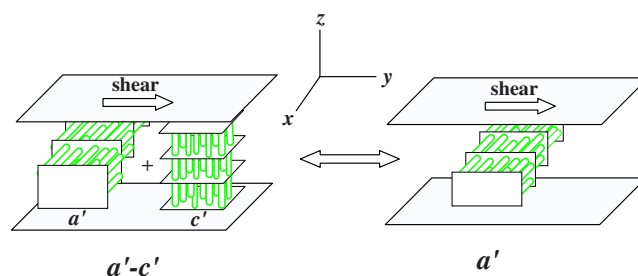


FIG. 1. (Color online) Schematic drawing of shear-induced a' - c' and a' structures in the S_A phase of 8CB. The a' - c' structure, which is a mixture of a' and c' structures, is stable at lower shear rates, while at higher shear rates the a' structure is stable.

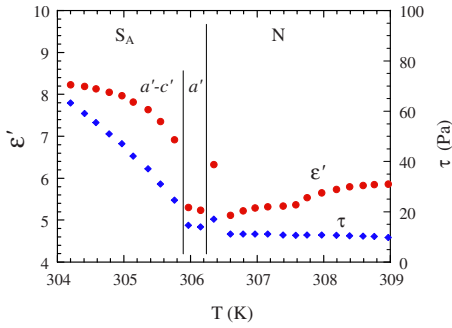


FIG. 2. (Color online) Temperature dependence of the shear-modified dielectric permittivity and the shear stress measured at a shear rate of 329.5 s^{-1} . When decreasing the temperature in the S_A phase, the a' structure changes to the $a'-c'$ structure. The peak just above the S_A phase is due to the a_c structure in the N phase.

mittivity and loss, a small voltage (5 V, 1 kHz) from an oscillator (FC110, YEW, Japan) was applied to the gap between the inner and the outer cylinders, and a phase sensitive detection of the current passing through the specimen was made with a lock-in amplifier (LI5640, NF, Japan). Owing to this geometry of the dielectric measurements, the observed dielectric constants correspond to those along the velocity gradient direction. The temperature of the specimen was controlled to within 0.05 K, using a temperature controller (340, Lakeshore, USA) and a heater and a thermocouple attached to the outer cylinder.

III. RESULTS AND DISCUSSION

Figure 2 shows the temperature dependence of the shear stress and the dielectric permittivity measured in the temperature region near the S_A - N phase transition point (T_{AN}). These measurements are made at a shear rate of 329.5 s^{-1} . With a decrease in temperature from the S_A - N phase transition point (T_{AN}), the shear stress is almost constant down to a temperature T_c , followed by a gradual increase below this temperature. Similar temperature dependence is observed in the dielectric permittivity except below T_c , where the dielectric permittivity tends to saturate at lower temperatures. These behaviors can be understood if we refer to the result of the x-ray scattering [10]; the a' structure is induced between T_c and T_{AN} and the $a'-c'$ structure below T_c . Here, a small peak just above T_{AN} observed both in the shear stress and the dielectric permittivity is due to the a_c structure in the N phase. In the a_c region, a precession of the director occurs around the neutral direction with its motion largely deviating along the velocity gradient direction [10], which is responsible for these peaks [15].

The $a'-c'$ and the a' regions are altered if the shear rate is varied. In Fig. 3, the temperature dependence of the shear stress and the dielectric permittivity when varying the shear rate is given. As obvious from these figures, at lower shear rates, the a' region becomes narrower with its region shifting to higher temperature and the $a'-c'$ region starts at higher temperatures. The change is also recognized in the N phase; lower shear rate makes the a_c region, which is specified by the peak, ambiguous and shift to higher temperatures. Based

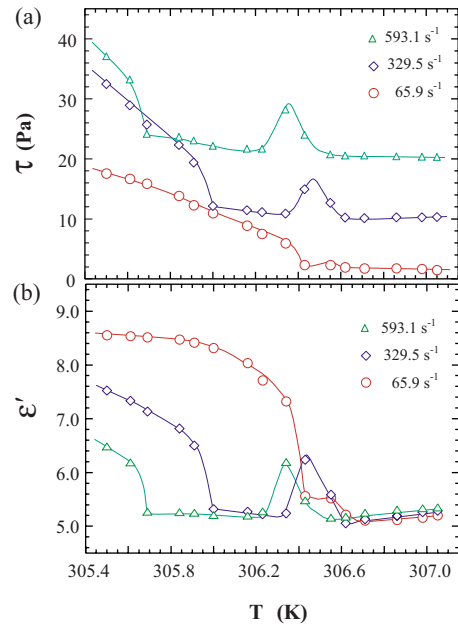


FIG. 3. (Color online) Temperature dependence of (a) the shear stress and (b) the dielectric permittivity at some shear rates. Lines are guide for eyes. With increase in the shear rate, the a' region expands and the transition temperature from a' to $a'-c'$ structure shifts to lower temperatures.

on such measurements, shear diagram, which specify the stable regions of the shear-induced structures in the shear rate vs the temperature space, is determined. As shown in Fig. 4, the transition temperatures from a_c to a' and that from a' to $a'-c'$ decrease almost linearly when increasing the shear rate with the latter showing larger shear rate dependence. It is also recognized that at lower shear rates the a' region disappears. The shear diagram thus obtained is almost similar to that obtained by Safinya *et al.* [10]. In their diagram, however, the transition temperature from the a_c to the a' region increases with the shear rate below $\sim 300 \text{ s}^{-1}$, which is not recognized in our result.

When measuring the shear stress as a function of shear rate, we changed the shear rate stepwise with an increment of 32.95 s^{-1} and monitored its response (time dependence of

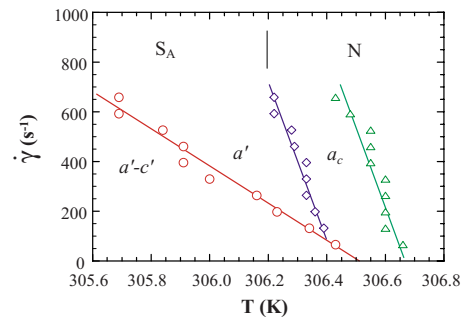


FIG. 4. (Color online) Shear diagram specifying the stable regions of the shear-induced structures. Lines are guide for eyes. With increase in the shear rate, the transition temperatures from a_c to a' structure and from a' to $a'-c'$ structure shift to lower temperatures with slope of the former being smaller than that of the latter. The a' region disappears at lower shear rates.

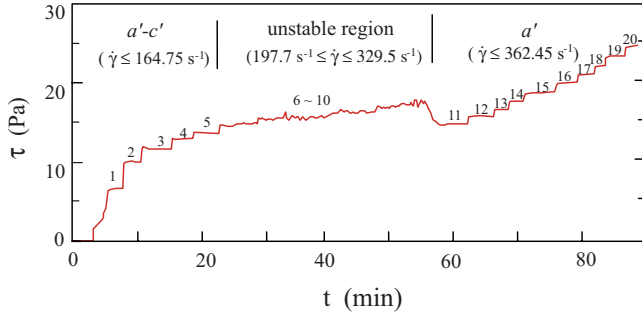


FIG. 5. (Color online) Time dependence of the shear stress when the shear rate is varied stepwise with an increment of 32.95 s^{-1} . The measurement is made at 306.0 K in the S_A phase. Integer n (1–20) is used to represent the shear rate ($n \times 32.95 \text{ s}^{-1}$) employed at each step. In the non-Newtonian $a'-c'$ ($\dot{\gamma} \leq 164.75 \text{ s}^{-1}$) and Newtonian a' ($\dot{\gamma} \geq 362.45 \text{ s}^{-1}$) regions, the shear stress after the shear rate change becomes constant in a short period of time. At the shear rates between 197.7 and 329.5 s^{-1} , unstable flow is recognized, characterized by noisy and drifting behavior.

the shear stress) on the recorder. A result in the S_A phase (306.0 K) is given in Fig. 5, where integer n (1–20) is used to represent the shear rate ($n \times 32.95 \text{ s}^{-1}$) employed at each step. This figure shows that in the a' region ($\dot{\gamma} \leq 164.75 \text{ s}^{-1}$) the shear stress after the stepwise shear rate change becomes constant in a short period of time (a few minutes) with its value not proportional to the shear rate (non-Newtonian flow), but between 197.7 and 329.5 s^{-1} the shear stress after the shear rate change does not become constant, accompanied by a large fluctuation, showing that the flow in this shear rate region is unstable. In the $a'-c'$ region ($\dot{\gamma} \geq 362.45 \text{ s}^{-1}$), the shear stress becomes constant in a short time again with its value proportional to the shear rate (Newtonian flow). Such a behavior is obtained at other temperatures in the S_A phase, showing that with increase in the shear rate the fluidity in the S_A phase changes from non-Newtonian ($a'-c'$ region) to Newtonian (a' region) via an unstable flow.

To make such a shear-rate-dependent flow clear, varying the temperature, the shear stress and the dielectric permittivity were simultaneously measured as functions of shear rate in the S_A phase ($T \leq 306.3 \text{ K}$). The results are given in Figs. 6(a) and 6(b), respectively, with the data in the unstable region specified by gray symbols. As is obvious from Fig. 6(a), a nonlinear relationship between the shear stress and the shear rate is obtained in $a'-c'$ and similar but somewhat fluctuated one in the unstable regions. In the a' region a linear relationship is obtained. In this figure, critical shear rate at which the flow becomes Newtonian is specified by arrows, showing that it shifts higher when decreasing the temperature. The critical change is also observed in the dielectric permittivity as given in Fig. 6(b). With increasing the shear rate, the dielectric permittivity decreases regularly in the $a'-c'$ region and somewhat irregularly in the unstable region, while in the a' region it becomes almost constant.

To clarify the nature of the $a'-c'$ structure, varying the shear rate, the frequency dependence of shear-modified dielectric permittivity and loss was measured at 305.8 K . The result of the dielectric permittivity is given in Fig. 7, show-

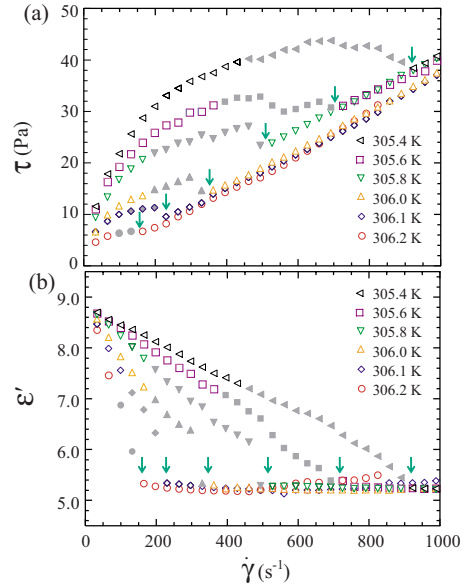


FIG. 6. (Color online) Shear rate dependence of (a) the shear stress and (b) the shear-modified dielectric permittivity at some temperatures in the S_A phase. The data in the unstable flow region are specified by gray symbols. The critical shear rate, at which the non-Newtonian flow ($a'-c'$ and unstable regions) changes to Newtonian flow (a' region), is indicated by arrow, showing that the critical shear rate increases when lowering the temperature. It is suggested that these behaviors are understood if we consider that the $a'-c'$ structure corresponds to shear-induced undulation (Fig. 9).

ing that a clear dielectric dispersion is recognized in the $a'-c'$ region (65.9 , 131.8 , and 197.7 s^{-1}), but not in the a' region (659.0 s^{-1}). In the unstable region (329.5 and 395.4 s^{-1}), the data fluctuate, but a remnant of the dielectric dispersion is observed. On the other hand, the dielectric loss largely increases at lower frequencies due to the contribution from the dc conductivity (σ), $\epsilon'' = \sigma / (\epsilon_0 \omega)$, as depicted in Fig. 8, where a result in the $a'-c'$ region at 65.9 s^{-1} is given as a representative one. The contribution from the dc conductivity (ϵ''_c) can be estimated from the plot of ϵ'' vs ω^{-1} . Using ϵ''_c thus estimated, $\Delta \epsilon'' = \epsilon'' - \epsilon''_c$ is derived and plotted together with ϵ'' in Fig. 8. As is obvious from this figure, a

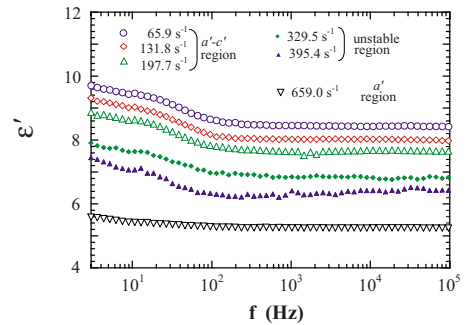


FIG. 7. (Color online) Frequency dependence of the shear-modified dielectric permittivity measured at some shear rates. The measurements are made at 305.8 K in the S_A phase. In the $a'-c'$ and unstable regions, a dielectric dispersion is recognized, while not in the a' region, indicating that the observed relaxation mode is a characteristic one induced in the $a'-c'$ and unstable regions.

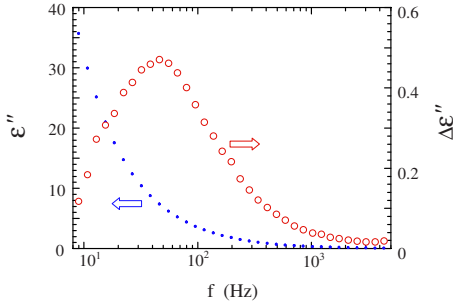


FIG. 8. (Color online) Frequency dependence of the shear-modified dielectric loss measured at a shear rate of 65.9 s^{-1} . The measurement is made at 305.8 K in the S_A phase. In the spectrum of $\Delta\epsilon''$, which is derived by subtracting ϵ_c (contribution from the dc conductivity) from ϵ'' , a peak is obtained. The relaxation time determined from the $\Delta\epsilon''$ peak is 3.5 ms. As suggested in the text, the shear-induced undulation is associated with this relaxation mode.

clear peak, which is related to the dielectric dispersion of ϵ' , is obtained. The relaxation time of this mode, which can be obtained from the peak frequency, is 3.5 ms. The $\Delta\epsilon''$ peak is also recognized in the unstable region with somewhat ambiguous behavior, but not in the a' region, indicating that the observed relaxation mode is a characteristic of the $a'-c'$ and the unstable regions.

To understand the relaxation mode described above and the mechanism of the shear-induced structural change in 8CB, some studies on the shear-induced undulation in the lamellar system are suggestive [17–22], of which recent non-equilibrium molecular-dynamics simulation by Guo [22] explains our results well. In his study, shear-induced parallel (c' structure) to perpendicular (a' structure) orientation change in the lamellar system is investigated and following results are obtained. In order to better understand this result, shear-induced structures are schematically drawn in Fig. 9, where cross section of each structure viewed from the shear flow direction (y axis) is given. (1) If a shear flow along the y direction is applied to the c' structure [Fig. 9(a)], an undulation instability is induced at lower shear rates with each layer undulating along the z direction [Fig. 9(b)]. With an increase in the shear rate, the viscosity decreases (non-

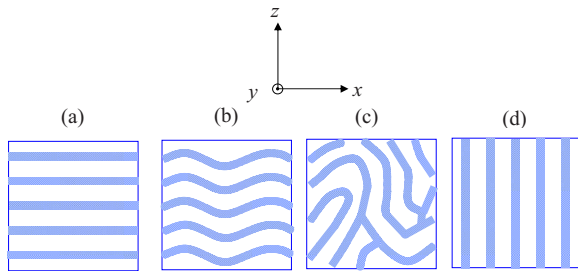


FIG. 9. (Color online) Schematic drawing of the shear-induced structures suggested from Guo's simulation [22]. If the shear flow along the y direction is applied to (a) the c' structure, (b) an undulation is induced with its displacement along the z axis. Further increase in the shear rate gives rise to (c) a chaotic structure, which has defects and lamellar domains, and subsequently to (d) simple a' structure. Our results are successfully understood in terms of such a structural change.

Newtonian flow) and the amplitude of the undulation grows. For the formation of the undulation, Auernhammer *et al.* [20] suggested that reduction in the layer spacing, which is caused by the shear-induced director tilting from the z axis, is responsible. (2) Further increase in the shear rate makes the undulation instability grow so large, and eventually at a certain shear rate defects are nucleated and the lamellar monodomain breaks into several lamellar domains with their layer normal randomly distributed in the zx plane [Fig. 9(c)]. (3) Subsequently, these domains merge into the monodomain a' structure energetically favored, leading to lower viscosity of this structure than that of the c' structure.

These results obtained from the simulation would give us a clue for understanding our observed results. As already mentioned, the $a'-c'$ structure suggested by Safinya *et al.* is not thoroughly characterized, i.e., how the a' structure mixes with the c' structure is not clarified. This can be resolved if we consider that the $a'-c'$ structure corresponds to the shear-induced undulation. The non-Newtonian flow in the $a'-c'$ region [Fig. 6(a)] can be successfully understood based on the shear-induced undulation. The behavior of the dielectric permittivity in the $a'-c'$ region [Fig. 6(b)] can also be explained in terms of the undulation which grows with increasing the shear rate. The dielectric permittivity in the liquid crystal is closely associated with the averaged values of the director components, since the dielectric permittivity in the liquid crystal is mainly determined by the orientation of the director. In the case of the undulation shown in Fig. 9(b), which is characterized by a director $(n_x, 0, n_z)$, averaged $\langle n_x \rangle$ and $\langle n_z \rangle$ are responsible for the macroscopic dielectric permittivity. If the amplitude of the undulation becomes larger with an increase in the shear rate, $\langle n_z \rangle$ changes from ~ 1 to ~ 0 , while $\langle n_x \rangle$ changes from ~ 0 to ~ 1 . Such changes in the director components would give rise to a decrease in the dielectric permittivity, since ϵ'_\parallel (ϵ' along the director) is larger than ϵ'_\perp (ϵ' perpendicular to the director) in 8CB [23], and ϵ' in the case of $\langle n_z \rangle = 1$ corresponds to ϵ'_\parallel , while ϵ' in the case of $\langle n_x \rangle = 1$ corresponds to ϵ'_\perp . The behavior of the dielectric permittivity in the $a'-c'$ region [Fig. 6(b)], thus, can be interpreted based on shear-assisted undulation growth, indicating that the $a'-c'$ structure corresponds to the shear-induced undulation. Further evidence for this correspondence is the shear-induced relaxation mode (Fig. 8). The dielectric dispersion of this mode can be recognized in the $a'-c'$ and the unstable regions with the relaxation time being a few ms, but not in the a' region. To identify the relaxation mode, the magnitude of the relaxation time is suggestive. It has been reported that the relaxation time of the undulation motion is on the order of 10^{-3} s [2,24], implying that the observed relaxation mode is due to the shear-induced undulation.

For the $a'-c'$ structure, another structure is proposed by Panizza *et al.* [16]. From the isotropic x-ray scattering pattern obtained from the plane (zx plane) perpendicular to the flow direction (y direction), it is suggested that the structure induced in this region consists of multilamellar cylinders elongated along the flow direction. This structure is also characterized by the director $(n_x, 0, n_z)$ compatible with the $a'-c'$ structure; however, the directors in the zx plane are aligned radially in the cylinder. Such an isotropic nature of the director in the zx plane is not affected by varying the

shear rate, indicating that the dielectric behavior in the $a'-c'$ region [Fig. 6(b)] cannot be explained in terms of the multilamellar cylinders. The multilamellar cylinders, thus, may be ruled out for the $a'-c'$ structure.

The unstable region observed between the $a'-c'$ and the a' structures can be regarded as the chaotic structure depicted in Fig. 9(c). The chaotic structure is not a definitive one with its structure varying with time, which would be responsible for the fact that the shear stress does not become constant in this region (Fig. 5). The somewhat ambiguous dielectric dispersion in this region (Fig. 7) can be understood in terms of the partially existing undulation. According to the Guo's simulation [22], the chaotic structure exists as an instantaneous step when the undulation transforms into the a' structure, without its existing region specified by the shear stress and the temperature. This is not incompatible with our result, for which further study would be necessary.

IV. SUMMARY

Simultaneous measurements of the rheological and the dielectric properties are made to clarify the shear-induced structural change in the S_A phase of 8CB. From the measurements of the shear stress and the dielectric permittivity as functions of temperature and the shear rate, shear diagram,

which specifies the stable regions of the shear-induced structures ($a'-c'$ and a' structures), is determined. The shear diagram thus obtained is similar to that reported by Safinya *et al.* [10]. In the measurement of the shear rate dependence of the shear stress, changes in fluidity are recognized; with an increase in the shear rate, non-Newtonian flow in the $a'-c'$ region changes to Newtonian flow in the a' region via an unstable flow region. In the simultaneously measured dielectric permittivity, characteristic shear rate dependence compatible with the rheological result is obtained; the dielectric permittivity decreases with an increase in the shear rate in the $a'-c'$ and the unstable regions and becomes constant in the a' region. In addition, from the frequency dependence of the dielectric permittivity, it is found that a relaxation mode appears in the $a'-c'$ and the unstable regions with the relaxation time being a few ms, but not in the a' region. Based on these results and Guo's simulation [22], it is indicated that the $a'-c'$ structure suggested from the x-ray scattering experiment corresponds to shear-induced undulation, and that the results obtained in the present study are successfully interpreted based on the structural changes associated with the shear-induced undulation; with an increase in the shear rate, the shear-induced undulation transforms to a more simple a' structure (perpendicular structure) via a chaotic structure.

-
- [1] P. G. de Gennes and J. Prost, *The Physics of Liquid Crystals*, 2nd ed. (Oxford University Press, New York, 1993).
- [2] S. Chandrasekhar, *Liquid Crystals*, 2nd ed. (Cambridge University Press, Cambridge, England, 1992).
- [3] Ch. Gähler, Phys. Rev. Lett. **28**, 1554 (1972).
- [4] K. Negita, J. Chem. Phys. **105**, 7837 (1996).
- [5] F. M. Leslie, Q. J. Mech. Appl. Math. **19**, 357 (1966).
- [6] J. L. Ericksen, Arch. Ration. Mech. Anal. **4**, 231 (1960).
- [7] K. Negita, J. Chem. Phys. **125**, 144517 (2006).
- [8] T. Carlsson, Mol. Cryst. Liq. Cryst. **104**, 307 (1984).
- [9] T. Carlsson and K. Skarp, Mol. Cryst. Liq. Cryst. **78**, 157 (1981).
- [10] C. R. Safinya, E. B. Sirota, and R. J. Plano, Phys. Rev. Lett. **66**, 1986 (1991).
- [11] C. R. Safinya, E. B. Sirota, R. Plano, and R. F. Bruinsma, J. Phys.: Condens. Matter **2**, SA365 (1990).
- [12] K. Skarp, T. Carlsson, S. T. Lagerwall, and B. Stebler, Mol. Cryst. Liq. Cryst. **66**, 199 (1981).
- [13] K. Negita, Mol. Cryst. Liq. Cryst. **300**, 163 (1997).
- [14] K. Negita and S. Uchino, Mol. Cryst. Liq. Cryst. **378**, 103 (2002).
- [15] K. Negita, M. Inoue, and S. Kondo, Phys. Rev. E **74**, 051708 (2006).
- [16] P. Panizza, P. Archambault, and D. Roux, J. Phys. II **5**, 303 (1995).
- [17] M. Goulian and S. T. Milner, Phys. Rev. Lett. **74**, 1775 (1995).
- [18] R. Bruinsma and Y. Rabin, Phys. Rev. A **45**, 994 (1992).
- [19] A. G. Zilman and R. Granek, Eur. Phys. J. B **11**, 593 (1999).
- [20] G. K. Auernhammer, H. R. Brand, and H. Pleiner, Phys. Rev. E **66**, 061707 (2002).
- [21] Th. Soddemann, G. K. Auernhammer, H. Guo, B. Dünweg, and K. Kremer, Eur. Phys. J. E **13**, 141 (2004).
- [22] H. Guo, J. Chem. Phys. **124**, 054902 (2006).
- [23] B. P. Ratna and R. Shashidhar, Mol. Cryst. Liq. Cryst. **42**, 113 (1977).
- [24] R. Ribotta, D. Salin, and G. Durand, Phys. Rev. Lett. **32**, 6 (1974).